PRE-DFT TOMLINSON-HARASHIMA PRECODING FOR SC-FDMA

Mohamed Noune and Andrew Nix

Centre for Communications Research, University of Bristol
Merchants Ventures Building, Woodland Road, BS8 1TJ, Bristol UK
Email: {Mohamed.Noune,Andy.Nix}@bristol.ac.uk

ABSTRACT

There is considerable interest in the use of Single Carrier Frequency Division Multiple Access (SC-FDMA) as the uplink transmission scheme in the 3GPP Long Term Evolution standard. In this paper a pre-DFT time-domain implementation of Tomlinson-Harashima Precoding (THP) for uplink SC-FDMA is proposed. We demonstrate how precoding the uplink transmission is an alternative signal processing technique to equalization in order to combat the frequency selective nature of the propagation channel. We investigate the BER performance and PAPR characteristics of the precoded SC-FDMA waveform for ZF and MMSE criterion. Results reported here show that MMSE-THP offers a gain of 3-4 dB in SNR over a DFE with ideal feedback and approaches the matched filter bound.

1. INTRODUCTION

The significant expansion seen in mobile and cellular technology over the last two decades is a direct result of the increasing demand for high data rate transmissions over bandwidth and power limited wireless channels. This requirement for high data rates results in significant inter-symbol interference (ISI) for single carrier systems, and thereby requires the use of robust coding and powerful signal processing techniques in order to overcome the time and frequency selective natures of the propagation channel. In recent years Orthogonal Frequency Division Multiplexing (OFDM) has been proposed for a range of future standards [1]. This trend has occurred since OFDM offers high performance and low terminal complexity for high data rate transmissions over bandwidth and power limited wireless channels. Particular examples include the physical layer of high performance Wireless Local Area Networks (WLANs), such as the 802.11 family of standards [1]. For short range devices, despite the high peak-to-average power ratio (PAPR) of the OFDM signal [1], OFDM solutions are more common than their single carrier counterparts.

A working assumption in the 3GPP LTE standard is the use of Orthogonal Frequency Division Multiple Access (OFDMA) on the downlink and SC-FDMA on the uplink [6]. This is justified by the inherent single carrier structure of SC-FDMA, which results in reduced sensitivity to phase noise and a lower Peak-to-Average Power Ratio (PAPR) compared to Orthogonal Frequency Division Multiple Access (OFDMA). This, consequently, makes it more attractive for low cost devices with limited transmit power. SC-FDMA can be considered as an extension of Single-Carrier Frequency Domain Equalization (SC-FDE) [2], with a flexibility in resource allocation.

SC-FDMA can be used with a range of single carrier Frequency Domain Equalization (FDE) techniques to combat the frequency selective nature of the transmission channel. These include frequency-domain Linear Equalization (LE), Decision Feedback Equalization (DFE) and the more recent Turbo Equalization [3]. Decision Feedback Equalization (DFE) offers a performance that is superior to that of conventional LE because of its ability to cancel precursor echoes without noise enhancement. These equalizers are required to produce instantaneous decisions. When incorrect decisions are made, DFEs behave poorly due to error propagation. In order to overcome these shortcomings alternative schemes have been proposed. THP is an effective way to account for the error propagation problem in a DFE since its feedback filter is implemented at the transmitter and is thus error free [4]- [5]. The dynamic range of the precoded waveform increases in the presence of deep channel fades [7]. To reduce this problem THP is implemented with a modulo operator. Since the operation of THP is tightly connected to the modulated signal constellation, and since the transmitted SC-FDMA signal does not have a distinct constellation, we propose a pre-DFT implementation of THP in this paper.

This paper is organized as follows. In section 2 the SC-FDMA transmission model is provided followed by an overview of the pre-DFT THP in section 3. In section 4 we derive the coefficients of the pre-DFT implementations of THP. Section 5 presents a comparison between the Complementary Cumulative Density Function (CCDF) of the PAPR for each scheme as well as it BER performance. Conclusions are presented in section 6.

2. SC-FDMA SYSTEM MODEL

Figure 1 shows the structure of the uplink SC-FDMA system considered in this paper. The variables in Figure 1 are defined in this section.

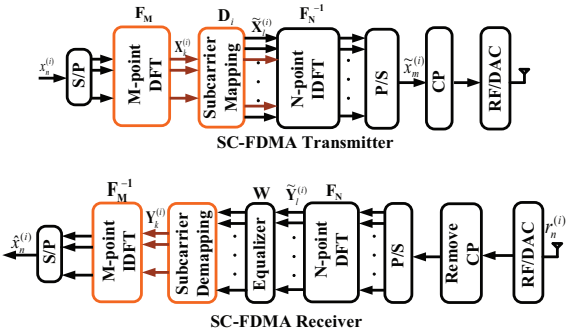

Figure 1: Transmitter structure for SC-FDMA.

For the i-th user, and for each block of M data samples, $\mathbf{x}^{(i)}$ with elements $x_m^{(i)}$, the transmitter maps the corresponding M frequency components of the block, $\mathbf{X}^{(i)}$ with elements $X_k^{(i)}$, resulting from an $M-$point DFT of the data samples, onto a set of M active sub-carriers selected from a total of N sub-carriers, where $N = QM$ and Q is the number of resource units. We denote Ψ_i as the set of sub-carriers occupied by the i-th user. The remaining $N-M$ sub-carriers are in-active since they are used by other uplink users.
We denote the sub-carrier mapping transform matrix for the i-th user by $\mathbf{D}_i$. $\mathbf{D}_i$ satisfies:

$$\mathbf{D}_j^T \mathbf{D}_i = \begin{cases} \mathbf{I}_M & j = i \\ \mathbf{0}_{M\times M} & j \neq i \end{cases} \quad (1)$$

The sub-carrier mapping produces $\widetilde{\mathbf{X}}^{(i)} = \mathbf{D}_i \mathbf{X}^{(i)}$. $\widetilde{\mathbf{X}}^{(i)}$ is processed by the N-point Inverse DFT (IDFT) to produce the time-domain transmitted signal $\widetilde{\mathbf{x}}^{(i)}$ with elements $\widetilde{x}_n^{(i)}$. The SC-FDMA transmitted signal can be represented by:

$$\widetilde{\mathbf{x}}^{(i)} = \mathbf{C}\mathbf{F}_N^{-1}\mathbf{D}_i\mathbf{F}_M\mathbf{x}^{(i)} \tag{2}$$

where $\mathbf{F}_N^{-1}$ and $\mathbf{F}_M$ are the N-point IDFT and M-point DFT matrix respectively. $\mathbf{C}$ represents the CP insertion matrix.

The received signal $r_n^{(i)}$ at time n for the SC-FDMA system operating in a multipath fading channel corrupted by Additive White Gaussian Noise, $w_n^{(i)}$, with variance σ_n^2, is given by:

$$r_n^{(i)} = \sum_{k=0}^{L} h_k \widetilde{x}_{n-k}^{(i)} + w_n^{(i)} \tag{3}$$

After removing the CP at the receiver, the received signal $\mathbf{r}^{(i)}$ can be described as:

$$\begin{aligned} \mathbf{r}^{(i)} &= \mathbf{H}\widetilde{\mathbf{x}}^{(i)} + \mathbf{w}^{(i)} \\ &= \mathbf{F}_N^{-1}\overline{\mathbf{H}}\mathbf{F}_N\mathbf{F}_N^{-1}\mathbf{D}_i\mathbf{F}_M\mathbf{x}^{(i)} + \mathbf{w}^{(i)} \\ &= \mathbf{F}_N^{-1}\overline{\mathbf{H}}\mathbf{D}_i\mathbf{F}_M\mathbf{x}^{(i)} + \mathbf{w}^{(i)} \end{aligned} \tag{4}$$

where $\mathbf{H}$ is a circulant channel matrix, $\mathbf{w}$ is a column vector containing complex AWGN noise samples, and $\overline{\mathbf{H}}$ is a diagonal matrix whose entries are generated from the N-point DFT of the channel impulse response. The received data samples are then given by:

$$\begin{aligned} \widehat{\mathbf{x}}^{(i)} &= \mathbf{F}_M^{-1}\mathbf{D}_i^T\mathbf{F}_N\mathbf{r}^{(i)} \\ &= \mathbf{F}_M^{-1}\mathbf{D}_i^T\overline{\mathbf{H}}\mathbf{D}_i\mathbf{F}_M\mathbf{x}^{(i)} + \mathbf{w}' = \mathbf{H}'\mathbf{x}^{(i)} + \mathbf{w}' \end{aligned} \tag{5}$$

where $\mathbf{w}'$ is the effective additive noise after receiver processing with samples:

$$w_m' = \frac{1}{M}\sum_{k\in\Psi_i}\left(\sum_{n=0}^{N-1} w_n e^{-j2\pi\frac{nk}{N}}\right)e^{j2\pi\frac{mk}{M}} \tag{6}$$

$\mathbf{H}'$ is a circulant matrix of the resultant channel impulse between the transmit and received SC-FDMA data symbols. This resultant channel impulse can be obtained by converting the channel frequency response on the i-th user's sub-carriers to the time-domain:

$$h_l' = \frac{1}{M}\sum_{k\in\Psi_i}\left(\sum_{n=0}^{L} h_n e^{-j2\pi\frac{nk}{N}}\right)e^{j2\pi\frac{lk}{M}},\ l = 0,\cdots,M-1 \tag{7}$$

we can therefore write equation (5) as:

$$\widehat{x}_n^{(i)} = \sum_{l=0}^{M-1} h_l' x_{n-l}^{(i)} + w_n' \tag{8}$$

This shows that the equivalent channel response spans the entire block of M data samples and this is a result of the energy leakage from the combined transmitter and receiver DFT processing.

In order to illustrate the energy leakage of the equivalent channel impulse response, we calculate the percentage of the energy concentration in the first L taps of the equivalent channel. Figure 2 shows the energy concentration metric of the equivalent channel for four different resource units with Localized SC-FDMA processing of a typical 16-tap non line-of-sight urban channel generated from the Spatial Channel Model (SCM) [9]. The total number of sub-carriers is N=512 and it was assumed that each user occupies M=128 sub-carriers. As can be seen, for each resource block more than 80% of the energy of h' is concentrated in the first four taps, whereas most of the energy is concentrated in the last two taps. This means that, indeed, the receiver processing results in time domain leakage of the channel impulse response.

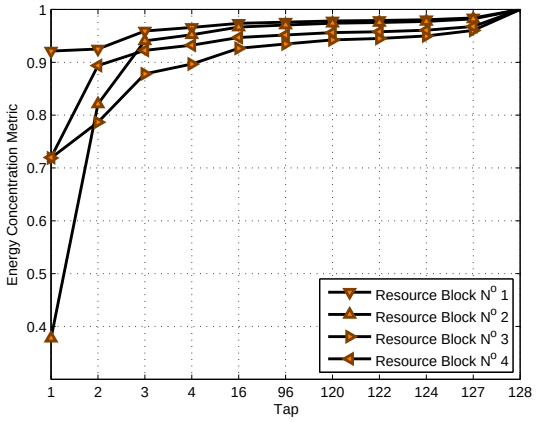

Figure 2: Energy Concentration Metric for the Equivalent Channel under L-FDMA

3. PRE-DFT THP

Here we consider the Tomlinson-Harashima precoder combined with single-carrier Frequency-Domain Equalization (SC-FDE) for uplink SC-FDMA. THP is an effective way to account for the error propagation problem in the DFE, since the feedback filter can be implemented at the transmitter. As shown in equation (8), the THP filtering can be applied directly to the data samples x_n. We refer to this scheme as the pre-DFT THP since the THP filtering is applied to the input of the M-point DFT in the SC-FDMA transmitter. The structure of the pre-DFT THP is shown in Figure 3(a). The operation of the TH-Precoder is described in [4]- [5]. The pre-DFT THP consists of an N_b-order feedback filter, a modulo operator at the transmitter and an M tap frequency-domain equalizer at the receiver with weights G_k. The length of the THP filter, N_b, is set to match the length of the resultant channel memory. Since the complexity of the THP (number of complex multiplications and complex additions) is related to the number of taps N_b, setting $N_b = M-1$ will result in a highly complex precoder, which is not desirable for user terminals. We will assume that the length of the THP filter is $N_b = L'$.

As a result of precoding the dynamic range of the precoded waveform increases, especially for channels experiencing deep fades. This increases the PAPR of the transmitted waveform. In order to overcome this limitation the THP is implemented with a modulo device. The modulo operation aims to reduce the dynamic range of the precoded waveform, regardless of the precoder's coefficients. For an K^2-QAM constellation, the output of the modulo operation is:

$$x_n = z_n - 2K\left\lfloor\frac{\Re(z_n)}{2K}+\frac{1}{2}\right\rfloor - j2K\left\lfloor\frac{\Im(z_n)}{2K}+\frac{1}{2}\right\rfloor \tag{9}$$

where $\Re(\bullet)$ and $\Im(\bullet)$ denote the real and imaginary parts respectively. $\lfloor\bullet\rfloor$ denotes the flooring operation.
The precoder's output is given by:

$$y_n = x_n - \sum_{m=1}^{N_b} b_m y_{n-m} \tag{10}$$

where the K^2-QAM symbol x_n is the precoder's input and b_m are the filter coefficients. If we re-arrange both sides of equation (10) and take the M-point DFT of both sides of this equation we obtain:

$$X_k = \left(1 + \sum_{n=1}^{N_b} b_n e^{-j2\pi\frac{kn}{M}}\right)Y_k = B_k Y_k \tag{11}$$

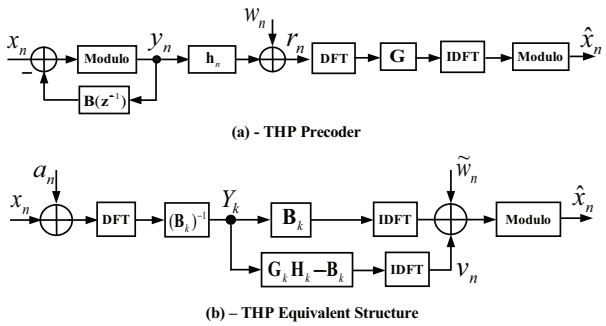

Figure 3: Tomlinson-Harashima Precoder

where $B_k = \left(1 + \sum_{n=1}^{N_b} b_n e^{-j2\pi\frac{kn}{M}}\right)$. The precoder's output $\mathbf{y}$ can be expressed in matrix form as:

$$\mathbf{x} = \begin{bmatrix} 1 & 0 & \cdots & 0 & b_L & \cdots & b_1 \\ b_1 & \ddots & \ddots & \vdots & \ddots & \ddots & \vdots \\ \vdots & \ddots & 1 & 0 & \cdots & 0 & b_L \\ b_L & \cdots & b_1 & 1 & 0 & \cdots & 0 \\ 0 & \ddots & \vdots & b_1 & 1 & \ddots & \vdots \\ \vdots & \ddots & b_L & \vdots & \ddots & \ddots & 0 \\ 0 & \cdots & 0 & b_L & \cdots & b_1 & 1 \end{bmatrix} \mathbf{y} = \overline{\mathbf{B}}\mathbf{y} \qquad (12)$$

where $\overline{\mathbf{B}}$ is a circulant matrix. Combining equations (2) and (12) leads to:

$$\mathbf{y} = \overline{\mathbf{B}}^{-1}\mathbf{x} = \mathbf{P}\mathbf{x} \qquad (13)$$

where $\mathbf{P}$ is the precoding matrix. Since the inverse of a circulant matrix is a circulant matrix, the pre- and post- multiplication of $\mathbf{P}$ by the M-point DFT and IDFT matrices, respectively, produces Π, a diagonal matrix containing the eigenvalues of $\mathbf{P}$, which are the DFT of the first row $\mathbf{P}$:

$$\mathbf{y} = \left(\mathbf{F}_M^{-1}\Pi\mathbf{F}_M\right)\mathbf{x} \qquad (14)$$

4. THP COEFFICIENTS

The transmitter requires full knowledge of the uplink channel in order to perform precoding. For TDD systems, as long as the time slot duration of the combined uplink and downlink transmission is less than the coherence time of the time-varying fading channel, the channel coefficients can be calculated at the BS during the uplink transmission and sent back to the resource unit. Thus, in this paper we assume that channel estimation is performed at the BS, where the mean of the wideband channel is normalized to unity and the channel information is sent back to the mobile unit.

The derivation of the THP coefficient calculation is given in [8]. The length of the precoder filter is set to match the length of the channel memory to ensure that all the ISI from the previous symbols are cancelled. The output of frequency-domain equalizer (FDE) at the receiver is given by:

$$\widehat{x}_n = \frac{1}{M}\sum_{k\in\Psi_i} G_k H_k Y_k e^{j2\pi\frac{kn}{M}} + \widetilde{w}_n \qquad (15)$$

where the k-th sub-carrier of the frequency-domain equalizer weights, the received signal and the additive noise, are denoted by G_k, R_k and W_k respectively. $\widetilde{w}_n$ is the filtered noise at the output of the FDE. Combining equations (11) and (15) produces:

$$\begin{aligned}\widehat{x}_n &= \frac{1}{M}\sum_{k\in\Psi_i}\left[\left(G_k H_k - B_k\right)Y_k + X_k\right]e^{j2\pi\frac{kn}{M}} + \widetilde{w}_n \\ &= x_n + \underbrace{\frac{1}{M}\sum_{k\in\Psi_i}\left(G_k H_k - B_k\right)Y_k e^{j2\pi\frac{kn}{M}}}_{=v_n} + \widetilde{w}_n \end{aligned} \qquad (16)$$

The error sequence of the pre-DFT THP, $e_n = \widehat{x}_n - \widetilde{x}_n$ where v_n is the residual interference in the current symbol decision. This shows that the output of the FDE is composed of the filtered noise $\widetilde{w}_n$ from the FDE, and the residual interference as a result of the precoder ($e_n = v_n + \widetilde{w}_n$), which is demonstrated in Figure 3(b).

4.1 ZF pre-DFT THP

The impulse response of the cascade of the discrete-time channel impulse response and the feedforward equalizer is the M-point IDFT of the product of H_k and G_k, as shown in equation (16), i.e:

$$u_n = \frac{1}{M}\sum_{k\in\Psi_i}\left(G_k H_k\right)e^{j2\pi\frac{kn}{M}}, \qquad n = 0,\cdots,N_b \qquad (17)$$

Under the Zero Forcing (ZF) criterion, from [7] and [8], all interference must be cancelled by the THP. As a result, the precoder's coefficients under the ZF criterion must be chosen such that $b_n = u_n$. From equation (17), the coefficients of the FDE must satisfy:

$$G_k = \frac{1}{H_k}\sum_{n=0}^{N_b} u_n e^{-j2\pi\frac{kn}{M}} = \frac{1}{H_k}\left(1 + \sum_{n=1}^{N_b} b_n e^{-j2\pi\frac{kn}{M}}\right) \qquad (18)$$

This means that the coefficients u_n can be chosen freely, which leads to computing the coefficients G_k and b_n. Here we choose the coefficient G_k such that the power of the filtered noise is minimized.
Let $\mathbf{b} = \left[b_1,\cdots,b_{N_b}\right]^T$. From [8], the precoder's coefficients satisfy $\mathbf{A}\mathbf{b} = -\mathbf{a}$, where:

$$[\mathbf{A}]_{m,l} = \sum_{k=0}^{M-1}\frac{e^{-j2\pi\frac{k(l-m)}{M}}}{\left|\overline{\mathbf{H}}_{k,k}\right|^2}, \; [\mathbf{a}]_m = \sum_{k=0}^{M-1}\frac{e^{j2\pi\frac{km}{M}}}{\left|\overline{\mathbf{H}}_{k,k}\right|^2}$$

where $\overline{\mathbf{H}}_{k,k}$ represents the k-th entry on the diagonal of $\overline{\mathbf{H}}$. with $1 \le m,l \le N_b$

4.2 MMSE pre-DFT THP

Under the MMSE criterion the coefficients of the FDE and precoder are chosen such that the sum of the power of the filtered noise, and the power of the residual interference are minimized. The cost function of the pre-DFT THP under the MMSE criterion is:

$$J_{\text{MMSE}} = \mathbf{E}\left[\|e_n\|^2\right] = \mathbf{E}\left[\left(v_n + \widetilde{w}_n\right)\left(v_n + \widetilde{w}_n\right)^H\right] \qquad (19)$$

where $\mathbf{E}[\bullet]$ denotes the expectation operator. Under the orthogonality principle, the precoder's output and the noise samples are uncorrelated and therefore $\mathbf{E}\left[v_n\widetilde{w}_n^H\right] = 0$. As shown in [8], the FDE coefficients satisfy:

$$G_k = \frac{H_k^* B_k}{|H_k|^2 + \frac{\sigma_n^2}{\sigma_s^2}} \qquad (20)$$

where σ_s^2 denotes the power of the signal x_n. The time-domain THP filter coefficients therefore satisfy $\mathbf{Ab} = -\mathbf{a}$, where:

$$[\mathbf{A}]_{m,l} = \sum_{k=0}^{M-1} \frac{e^{-j2\pi\frac{k(l-m)}{M}}}{\left|\overline{\mathbf{H}}_{k,k}\right|^2 + \frac{\sigma_n^2}{\sigma_s^2}}, \quad [\mathbf{a}]_m = \sum_{k=0}^{M-1} \frac{e^{j2\pi\frac{km}{M}}}{\left|\overline{\mathbf{H}}_{k,k}\right|^2 + \frac{\sigma_n^2}{\sigma_s^2}}$$

with $1 \leq m,l \leq N_b$.

4.3 Transmit Power Control

As a result of precoding, the mean transmit power per SC-FDMA symbol increases or decreases as a result of the magnitude fluctuations of the precoders weights. Since the transmit power per symbol is limited, we should maintain the same mean transmit power per symbol as the case with no precoding. Therefore, the weights of the precoder must be power constrained. For each precoded SC-FDMA symbol, the mean transmit power is given by:

$$\frac{1}{M}\sum_{k\in\Psi_i}\left|B_k^{-1}\widetilde{X}_k\right|^2 = \frac{\sigma_s^2}{M}\sum_{k\in\Psi_i}\left|B_k^{-1}\right|^2 = \gamma^2\sigma_s^2 \qquad (21)$$

where γ denotes the gain in the transmit power as a result of precoding and is given by $\gamma = \sqrt{\frac{1}{M}\sum_{k\in\Psi_i}\left|B_k^{-1}\right|^2}$. In order to normalize the transmit power to the case of no precoding, the precoders output is divided by γ. As a result of power normalization, the output of the FDE from equation (16) becomes:

$$\widehat{x}_n = \quad = \frac{1}{\gamma}x_n + \frac{1}{\gamma}\frac{1}{M}\sum_{k\in\Psi_i}(G_kH_k - B_k)Y_k e^{j2\pi\frac{kn}{M}} + \widetilde{w}_n \qquad (22)$$

This means that the power normalization at the transmitter results in a gain mismatch at the output of the receiver. Since we assume that the transmitter and receiver are perfectly synchronous and that the multipath channel is static and perfectly known at both sides of the link, in order to compensate for gain mismatch between the transmitter and receiver, the output of the receiver has to be multiplied by γ. Therefore, from equation (22):

$$\gamma\widehat{x}_n = \quad = x_n + \frac{1}{M}\sum_{k\in\Psi_i}(G_kH_k - B_k)Y_k e^{j2\pi\frac{kn}{M}} + \gamma\widetilde{w}_n \qquad (23)$$

Although multiplying the output of the FDE by γ restores the gain mismatch between the transmitter and receiver, it also results in noise enhancement. The implication of the noise enhancement is considered in section 5.

5. RESULTS AND DISCUSSION

This section presents a comparison of the simulation results for the DFE and THP for different SC-FDMA systems. In the simulation it is assumed that the sub-carrier bandwidth is 15kHz [6], the total number of available sub-carriers N = 512 and the number of user sub-carriers is M. The CP length is P = 64, which is longer than the channel delay spread. QPSK modulation and Localized sub-carrier mapping are assumed. For each value of Q, the number of resource blocks, the results are averaged over the different possible sub-carrier arrangements through Frequency-Hopping. The frequency selective channel is generated from the NLoS channel model in [9], and the fading process on each tap is assumed to be Rayleigh fading. Perfect channel knowledge at the transmitter is assumed. Channel estimation is performed at the base-station, where the mean of the instantaneous wideband channel is normalized to unity and the channel information is sent back to the mobile unit. This means that transmit precoding is not used to compensate for the fast power fluctuations in the channel mean power.

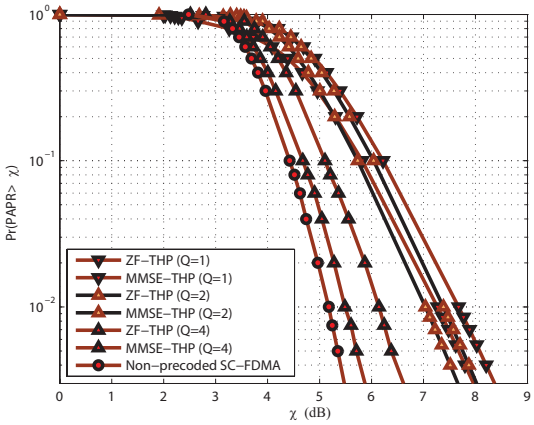

Figure 4: PAPR Characteristics of the precoded SC-FDMA waveform.

Figure 4 shows the CCDF of the PAPR for the ZF and MMSE THP waveforms for different values of M, calculated for each SC-FDMA symbol.As can be seen, the PAPR of the ZF-THP is higher than the PAPR of the MMSE-THP, for all M. This is as a result of the high dynamic range of the magnitudes of the ZF-THP compared to MMSE-THP. In addition, the PAPR of both schemes reduces as the number of active sub-carriers per user is reduces. Since SC-FDMA can be seen as DFT precoded OFDMA, smaller DFT sizes (smaller M) offer lower DFT spreads in the OFDMA modulator and hence the reduction in the PAPR of the precoded SC-FDMA waveform. This can be applied to widen the reach of the system, overcome the infrastructure penetration losses, and or lessen the power consumption of the transceiver, especially for low data rate transmissions, this is known as sub-channelization gain. For example, the 99% PAPR level (the PAPR level χ that satisfies Pr(PAPR$>\chi$)=0.01) for $Q = 4$ offers and improvement of 1dB compared $Q = 2$ and an improvement of almost 2dB compared to $Q = 1$ for both ZF and MMSE THP, which in addition to the sub-channelization gain offers a further improvement in the mean transmit power as Q grows larger (smaller M).

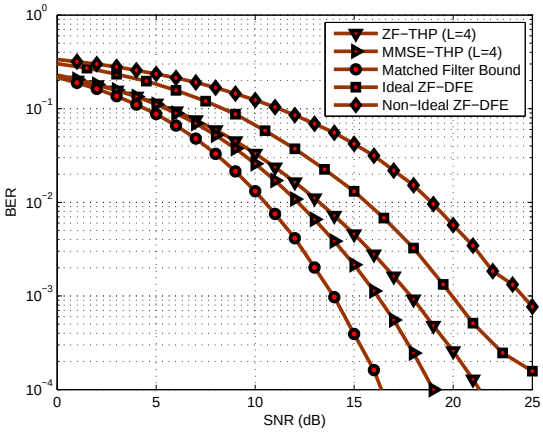

Figure 5: Uncoded BER Performance of ZF And MMSE THP for SC-FDMA system compared to ideal and non-ideal MMSE DFE for $Q = 4$ blocks.

Figure 5 shows the BER performance of the ZF- and MMSE-THP compared to ideal and non-ideal DFE for uncoded QPSK with four resource blocks. Both ZF and MSME THP outperform both the ideal-DFE (i.e. assuming perfect feedback decision) and the non-ideal DFE. The MMSE-THP offers a better BER performance compared to the ZF-THP since the MMSE-THP reduces the magnitude of the error resulting from both the residual ISI as a result of the combined channel and FDE, and the filtered additive noise, contrary to the ZF-THP, which only cancels the residual ISI.

Figures 6 and 7 show the ber performance of the MMSE and ZF pre-DFT THP, respectively, for different lengths of the precoder filter and different values of Q. From both figures, MMSE-THP outperforms ZF-THP. In addition, increasing the length of the precoder improves the performance for small values of N_b and degrades the performance as $N_b = M$ for both ZF and MMSE THP. The performance improvement for small values of N_b is due to the fact that increasing N_b permits the precoder, as shown in Figure 2, to cancel more ISI. As the length of the precoder is further increased, the precoder's gain γ increases and as a result when the receiver adjusts for the precoder's gain, noise enhancement occurs. This degradation in the performance, particularly when $N_b = M$, manifests itself as an irreducible BER floor.

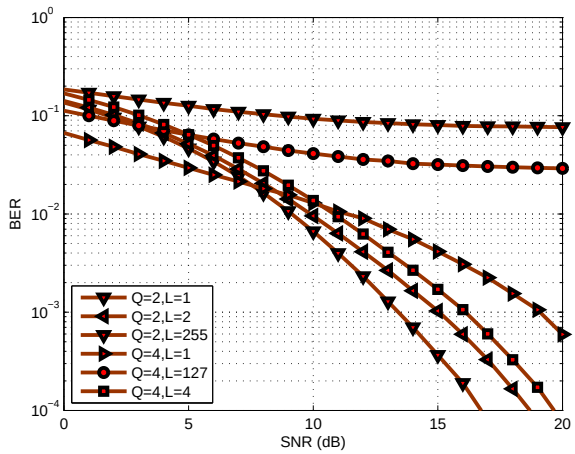

Figure 6: Uncoded BER Performance of SC-FDMA system with different blocks and MMSE-THP.

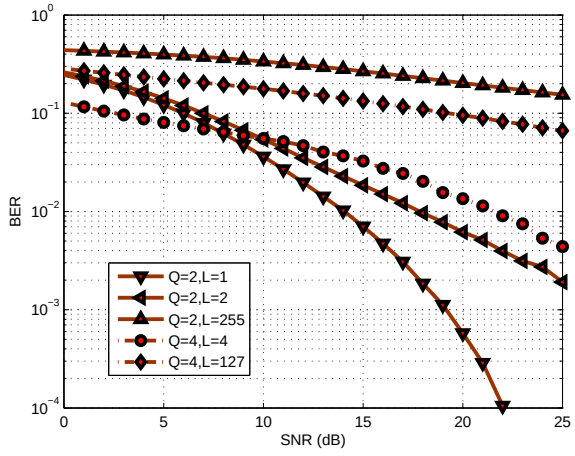

Figure 7: Uncoded BER Performance of SC-FDMA system with different blocks and ZF-THP.

6. CONCLUSION

Linear and Decision Feedback Equalization are two common assumptions in SC-FDMA. The former suffers from a fundamental performance degradation as a result of the residual ISI, while the latter suffers from performance degradation as a result of error propagation. To overcome these problems, in this paper we have presented a pre-DFT implementation of THP for uplink SC-FDMA transmission. Here we proposed the pre-DFT THP for SC-FDMA and both the ZF and MMSE THP designs were considered. The MMSE-THP offers a better BER performance compared to the ZF-THP, and also has a lower PAPR. Both systems offer a lower BER compared to decision feedback equalization and are close to the matched filter bound. Although precoding introduces a transmit power penalty as a result of the high PAPR (1.5dB for MMSE-THP and Q=4), the SNR gain of MMSE-THP compared to ideal-DFE exceeds this penalty (3.5 dB less SNR than ideal-DFE for Q=4 and an error probability $P_e = 10^{-3}$), which translates to improved coverage. As the number of taps in the THP filter, the BER performance of the precoded SC-FDMA system degrades as a result of the noise enhancement. Further work should address how channel estimation and tracking can assist the precoder in the case of channel mismatch due to mobility and channel estimation errors.

Acknowledgment

The authors would like to thank the Algerian Government for their financial support of this PhD, and the Centre for Communications Research for the provision of research facilities and access to a high performance computing cluster.

REFERENCES

[1] R. van Nee, and R. Prasad, "OFDM for Wireless Multimedia Communications", Norwood, MA: Artech House, 2000.

[2] David Falconer, S. Lek Ariyavisitakul, Anader Benyamin-Seeyar, Brian Eidson, "Frequency Domain Equalization for Single-Carrier Broadband Wireless Systems", Communications Magazine, IEEE, Apr. 2002.

[3] G. Berardinelli, B. E. Priyanto, T. B. Srensen, and P. Mogensen, "Improving SC-FDMA Performance by Turbo Equalization in UTRA LTE Uplink," IEEE Vehicular Technology Conference (VTC) 2008 Spring, Marina Bay, Singapore, May 2008.

[4] M. Tomlinson, "New automatic equalizer employing modulo arithmetic," Electron. Lett., vol. 7, pp. 138-139, Mar. 1971.

[5] H. Harashima and H. Miyakawa, "Matched-transmission technique for channels with intersymbol interference,"' IEEE Trans. Commun., vol. 20, pp. 774-780, Aug. 1972.

[6] Hyung G. Myung, Junsung Lim, and David J.Goodman, "Single Carrier FDMA for Uplink Wireless Transmission", 2006 IEEE Vehicular Technology Magazine 1 September 2006.

[7] R.D. Wesel, J.M. Cioffi, "Precoding and the MMSE-DFE", Proceedings of the 28th Asilomar Conference on Signals, Systems & Computers, 1995.

[8] N. Benvenuto and S. Tomasin, "On the Comparison between OFDM and Single-Carrier Modulation with a DFE Using a Frequency-Domain Feedforward Filter," IEEE Trans. Commun., vol. 50, no. 6, pp. 947-955, Jun. 2002.

[9] Final report on link level and system level channel Models, IST–2003–507581 WINNER D5.4 ver 1.4.